

Supporting Information

Diphenylamine Substituted 5,6,12,13-Tetraazaperopyrene based Polymorphic Microcrystals Versatile in Multi-directional Isotropic and Anisotropic Photon Transport

Di Tian,^a Chaofei Xu,^c Wei Yuan,^{a,b} Xue-Dong Wang*^c and Yulan Chen*^{a,b}

[a] Department of Chemistry, Tianjin Key Laboratory of Molecular Optoelectronic Science, Tianjin University, Tianjin, 300354, P. R. China

E-mail: yulanchen@jlu.edu.cn

[b] State Key Laboratory of Supramolecular Structure and Materials, College of Chemistry, Jilin University, Changchun, 130012, P. R. China

[c] Institute of Functional Nano & Soft Materials (FUNSOM), Jiangsu Key Laboratory for Carbon-Based Functional Materials & Devices, Soochow University, Suzhou, 215123, P. R. China

E-mail: wangxuedong@suda.edu.cn

Table of Contents

Experimental Procedures	1
1. Materials and characterizations	1
2. Preparation of c-TAPP-DPA crystals	1
3. Optical loss coefficient (R)	1
4. Experimental details	1
Results and Discussion.....	3
TGA curve (Figure S1).	3
Optical and electronic properties (Figure S2-S3, Table S1).....	3
Single crystal information (Figure S4-S6, Table S2-S4)	5
NMR spectra (Figure S7-S16)	7
Schematic demonstration of the experimental setup for optical waveguide characterization (Figure S17).....	12
References	12

Experimental Procedures

1. Materials and characterizations

General.

All chemicals and solvents were purchased from commercial sources and used without further purification unless noted otherwise. Dichloromethane (DCM) was distilled over CaH₂. Tetrahydrofuran (THF) was distilled over sodium and benzophenone.

Characterization.

¹H NMR (400 MHz) and ¹³C NMR (100 MHz) spectra were recorded on a 400 MHz Bruker AV400 spectrometer in CDCl₃. High-resolution mass spectra (HRMS) were obtained on a micrOTOF-QII mass spectrometer. UV-vis absorption spectra were obtained on a PerkinElmer Lambda 750 spectrophotometer. Fluorescence spectra were recorded on a Hitachi F-7000 fluorescence spectrophotometer. The absolute fluorescence quantum yield was measured by Edinburg FLS-980 fluorescence spectrometer with a calibrated integrating sphere. Cyclic voltammetry (CV) measurements were performed with a scan rate of 100 mV s⁻¹ on a CHI660E electrochemical analyzer, with 0.1 M tetrabutylammonium hexafluorophosphate (TBAPF₆) as supporting electrolyte, platinum as working and counter electrodes, and a standard calomel electrode (SCE) as reference electrode. Density functional theory (DFT) calculations were performed in Gaussian 09 software at the B3LYP functional with the 6-31G* basis set level. The single crystal X-ray diffraction was recorded on a Rigaku XtaLAB Synergy. Optical waveguide experiments were characterized by a home-built optical system (Figure S17).

2. Preparation of c-TAPP-DPA crystals

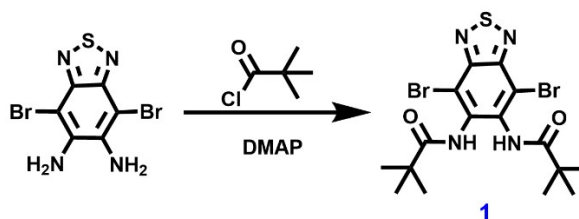
Geometrically well-defined 1D microrods and 2D rhomboid microplates of c-TAPP-DPA were cultivated by the solvent diffusion method at the liquid-liquid interface between methanol and DCM, or methanol and THF, respectively. In detail, 4 mL methanol was slowly injected into 1 mL DCM solution of c-TAPP-DPA (1 mg·mL⁻¹). After a period of time, the 1D microrods crystals were observed.

Hexagonal microplates were prepared by slow diffusion technique between methanol and THF. In detail, 1 mL THF solution of c-TAPP-DPA (1 mg·mL⁻¹) was placed in one vial, which was subsequently introduced into another vial containing 4 mL of methanol. The latter vial was closed, and after a period of time, the hexagonal microplates were observed.

3. Optical loss coefficient (*R*)

The optical loss coefficient (*R*) is the key parameter for evaluating optical waveguide performance. The value of the *R* was calculated by the formula $I_{body}/I_{tip} = A \times e^{(-RX)}$, where *I*_{body} and *I*_{tip} represent the intensity of light at the excitation point and output point, respectively; and *X* is the distance between the excited site and the output point.

4. Experimental details



4,7-Dibromo-2,1,3-benzothiadiazole-5,6-diamine was synthesized according to the literature procedures.^[1] To a dry DCM solution (50 mL) of 4,7-dibromo-2,1,3-benzothiadiazole-5,6-diamine (1.62 g, 5.00 mmol), triethylamine (5 mL) was added dropwise. And then a dry DCM solution (10 mL) of pivaloyl chloride (6.04 g, 50.00 mmol) was added dropwise to the mixture at 0 °C. After stirring at room temperature for 10 h, the solution was poured into water and extracted with DCM. The combined organic layers were dried over anhydrous MgSO₄ and evaporated to dryness. The residue was purified by chromatography on silica gel column (petroleum ether/ethyl acetate = 4/1) to afford **1** as a white solid (1.67 g, 68%). ¹H NMR (CDCl₃, 400 MHz): δ 8.07 (s, 2H), 1.38 (s, 18H). ¹³C NMR (CDCl₃, 100 MHz): δ 178.08, 151.62, 136.24, 112.69, 40.24, 28.06. ESI-TOF, m/z: calcd, 491.9648, found: 492.9718 ([M+H]⁺), 514.9536 ([M+Na]⁺).

A solution of **1** (0.49 g, 1.00 mmol), 4-(diphenylamino)phenylboronic acid (0.61 g, 2.10 mmol), Pd(PPh₃)₄ (161.80 mg, 0.14 mmol), aqueous Cs₂CO₃ (10.00 g, 16 mL, 32.00 mmol), PPh₃ (83.70 mg, 0.15 mmol), and aliquat 336 (2 drops) in toluene (48 mL) was heated at reflux for 12 h under nitrogen atmosphere. The mixture was cooled to room temperature and extracted with DCM. The combined organic extracts were dried with anhydrous MgSO₄ and evaporated to dryness. The residue was purified by chromatography on silica gel column (petroleum ether/ethyl acetate = 10/1 ~ 5/1) to afford **2** as a yellow solid (0.69 g, 84%). ¹H NMR (CDCl₃, 400 MHz): δ 7.90 (s, 2H), 7.41 (d, *J* = 8.6 Hz, 4H), 7.28 (t, *J* = 7.9 Hz, 8H), 7.20 (d, *J* = 8.6 Hz, 4H), 7.15 (d, *J* = 8.7 Hz, 8H), 7.06 (t, *J* = 7.5 Hz, 4H), 1.15 (s, 18H). ¹³C NMR (CDCl₃, 100 MHz): δ 177.46, 153.28, 148.15, 147.56, 133.03, 131.04, 129.48, 129.18, 128.00,

124.99, 123.48, 123.03, 39.66, 27.37. ESI-TOF, m/z: calcd, 820.3554, found: 821.3633 ([M+H]⁺), 843.3414 ([M+Na]⁺).

2 (0.50 g, 0.61 mmol), P₂O₅ (1.83g, 12.87 mmol) and POCl₃ (12 mL) were heated to reflux and stirred for 24 h under N₂. The mixture was cooled to room temperature and then added dropwise into NaOH solution (6 M), stirred for 30 min. The aqueous solution was adjusted to pH = 10, and filtered under reduced pressure. The residue was purified by chromatography on silica gel column (petroleum ether/ethyl acetate = 20/1) to afford **3** as an orange solid (57 mg, 12%). ¹H NMR (CDCl₃, 400 MHz): δ 10.36 (d, J = 9.2 Hz, 2H), 8.16 (s, 2H), 8.07 (d, J = 2.2 Hz, 2H), 7.78 (d, J = 9.4 Hz, 2H), 7.37 (t, J = 7.7 Hz, 8H), 7.28 (d, J = 7.7 Hz, 8H), 7.15 (t, J = 7.3 Hz, 4H), 1.64 (s, 18H). ¹³C NMR (CDCl₃, 100 MHz): δ 176.37, 146.92, 146.25, 145.79, 129.45, 129.08, 128.96, 126.49, 125.21, 123.92, 119.66, 117.95, 40.71, 31.15. ESI-TOF, m/z: calcd, 784.3343, found: 785.3416 ([M+H]⁺).

3 (200 mg, 0.25 mmol), zinc powder (330 mg, 5 mmol) were charged into a two-neck bottom, followed by addition of 10 mL of glacial acetic acid. After stirring at 100 °C for 3 min under N₂, the reaction was monitored by TLC until no starting material remained and cooled to room temperature. The reaction mixture was treated with distilled water (100 mL) at 0 °C. The mixture was extracted with DCM. The combined organic layers were dried over anhydrous MgSO₄ and evaporated to dryness. The crude product **4** (140 mg, 75%) was used in next step without further purification.

To a dry DCM solution (30 mL) of **4** (200 mg, 0.26 mmol), triethylamine (1 mL) was added dropwise. And then a dry DCM solution (5 mL) of pivaloyl chloride (2 mL) was added dropwise to the mixture at 0 °C. After stirring at room temperature for 10 h, the solution was poured into water and extracted with DCM. The combined organic layers were dried over anhydrous MgSO₄ and evaporated to dryness. The residue was purified by chromatography on silica gel column (petroleum ether/ethyl acetate = 5/1 ~ 3/1) to afford **5** as a white solid. ¹H NMR (CDCl₃, 400 MHz): δ 8.75 (d, J = 9.3 Hz, 2H), 8.51 (s, 2H), 8.07 (d, J = 2.2 Hz, 2H), 7.45 (d, J = 9.3 Hz, 2H), 7.34 (t, J = 7.9 Hz, 8H), 7.24 (d, J = 7.6 Hz, 8H), 7.12 (t, J = 7.3 Hz, 4H), 1.57 (s, 18H), 1.40 (s, 18H). ¹³C NMR (CDCl₃, 100 MHz): δ 176.80, 166.81, 147.61, 145.99, 139.59, 130.02, 128.80, 127.50, 126.95, 126.81, 125.60, 124.35, 123.89, 119.64, 119.45, 41.03, 40.24, 31.53, 28.38. ESI-TOF, m/z: calcd, 924.5085, found: 925.5156 ([M+H]⁺).

5 (250 mg, 0.27 mmol), P₂O₅ (1 g, 7.0 mmol) and POCl₃ (10 mL) were heated to reflux and stirred for 24 h under N₂. The mixture was cooled to room temperature and then added dropwise into NaOH solution (6 M), stirred for 30 min. The aqueous solution was adjusted to pH = 10, and filtered under reduced pressure. The residue was purified by chromatography on silica gel column (petroleum ether/ethyl acetate = 60/1) to afford **c-TAPP-DPA** as an orange solid (35 mg, 14%). ¹H NMR (CDCl₃, 400 MHz): δ 8.77(s, 4H), 7.37~7.47 (m, 16H), 7.21 (t, J = 6.7 Hz, 4H), 1.77 (s, 36H). ¹³C NMR (CDCl₃, 100 MHz): 167.87, 147.58, 145.72, 134.30, 130.24, 127.01, 125.80, 124.85, 124.62, 122.04, 113.30, 41.62, 31.35. ESI-TOF, m/z: calcd, 888.4874, found: 889.4954 ([M+H]⁺).

Results and Discussion

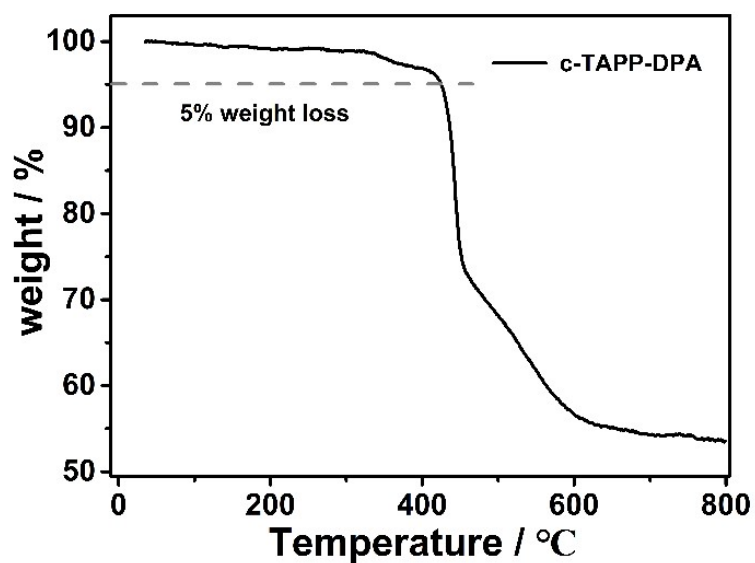


Figure S1. TGA trace of c-TAPP-DPA at a rate of $10\text{ }^{\circ}\text{C min}^{-1}$.

Optical and electronic properties

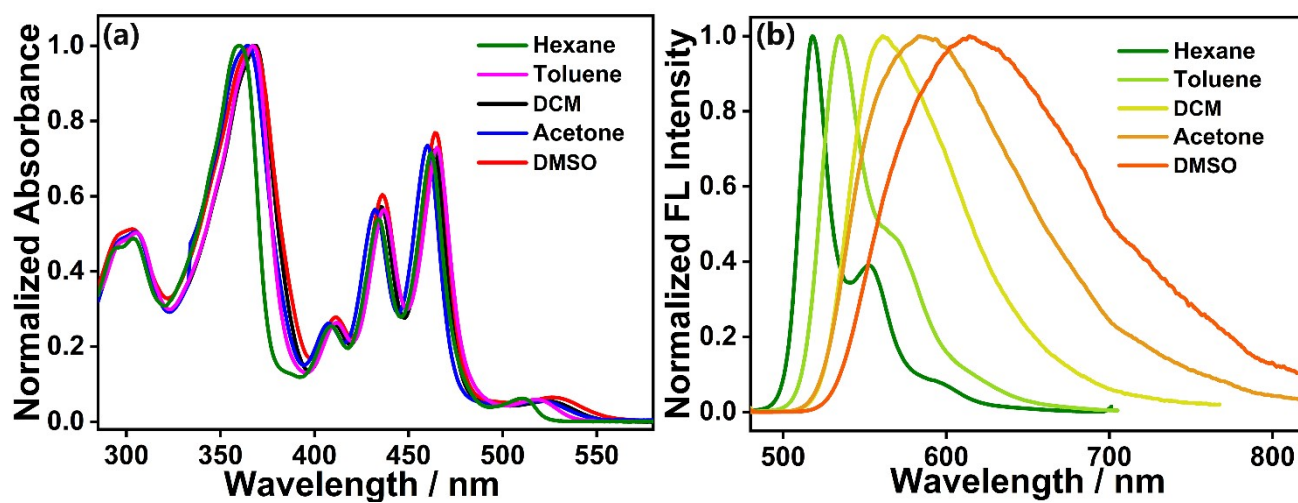
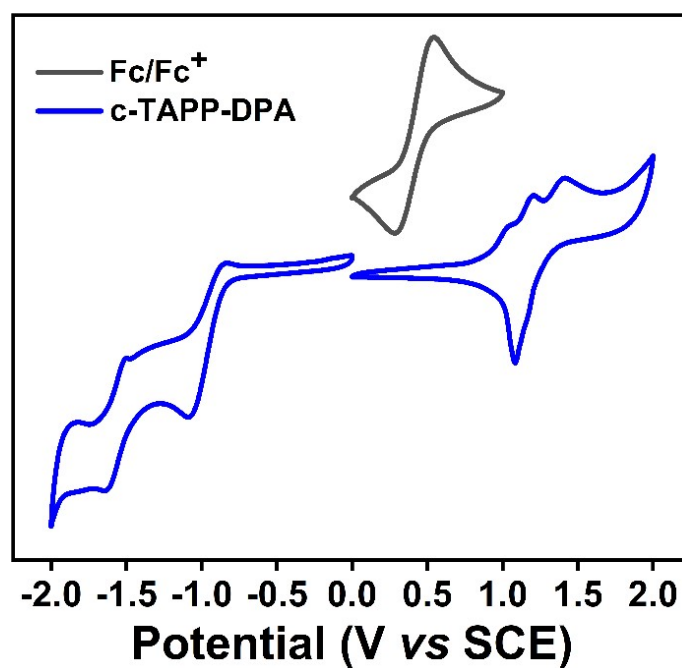


Figure S2. Normalized (a) UV-Vis absorption spectra and (b) FL emission spectra of c-TAPP-DPA in different solvents.

Table S1. Optical and electronic properties of **c-TAPP-DPA**.

c-TAPP-DPA	$\lambda_{abs}^{[a]}$ (nm)	$\lambda_{em}^{[a]}$ (nm)	PL Quantum Yield ^[b] (Φ_f)	$E_{ox}/E_{red}^{[c]}$ (eV)	$E_g^{[c]}$ (eV)	HOMO ^[c] (eV)	LUMO ^[c] (eV)
Solution/powder state	526	561	13.2% (s) / 42% (l)	+0.59/-1.14	1.73	-5.33	-3.60
Microrod	—	590	3.86%	—	—	—	—
Rhomboid microplate	—	590	3.87%	—	—	—	—
Hexagonal microplate	—	570	5.41%	—	—	—	—

^[a]The longest absorption and emission wavelength in DCM solution. ^[b]Absolute fluorescence quantum efficiency (Φ_f), determined using a calibrated integration sphere, s: solid; l: liquid. ^[c] E_g (electronic gap) estimated vs vacuum level from $E_{LUMO} = -(4.74 + E_{red})$, $E_{HOMO} = -(4.74 + E_{ox})$, E_{ox} and E_{red} were the onset potential of the first oxidation or reduction wave vs E_{Fc/Fc^+} .

**Figure S3.** Cyclic voltammograms of **c-TAPP-DPA** measured in DCM with 0.1 M TBAPF₆ as electrolyte (scan rate = 100 mVs⁻¹).

Single crystal information

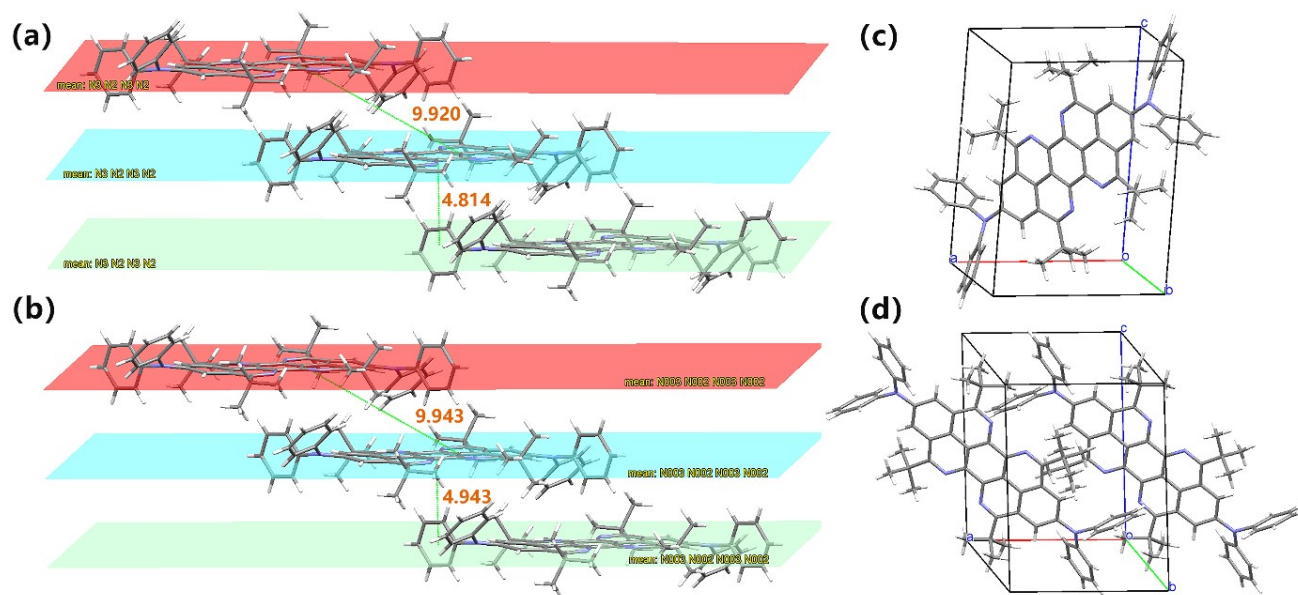


Figure S4. Molecular packing mode of a) 1D microrod b) 2D rhomboid microplate; The molecular packing arrangement in one unit cell of c) 1D microrod d) 2D rhomboid microplate.

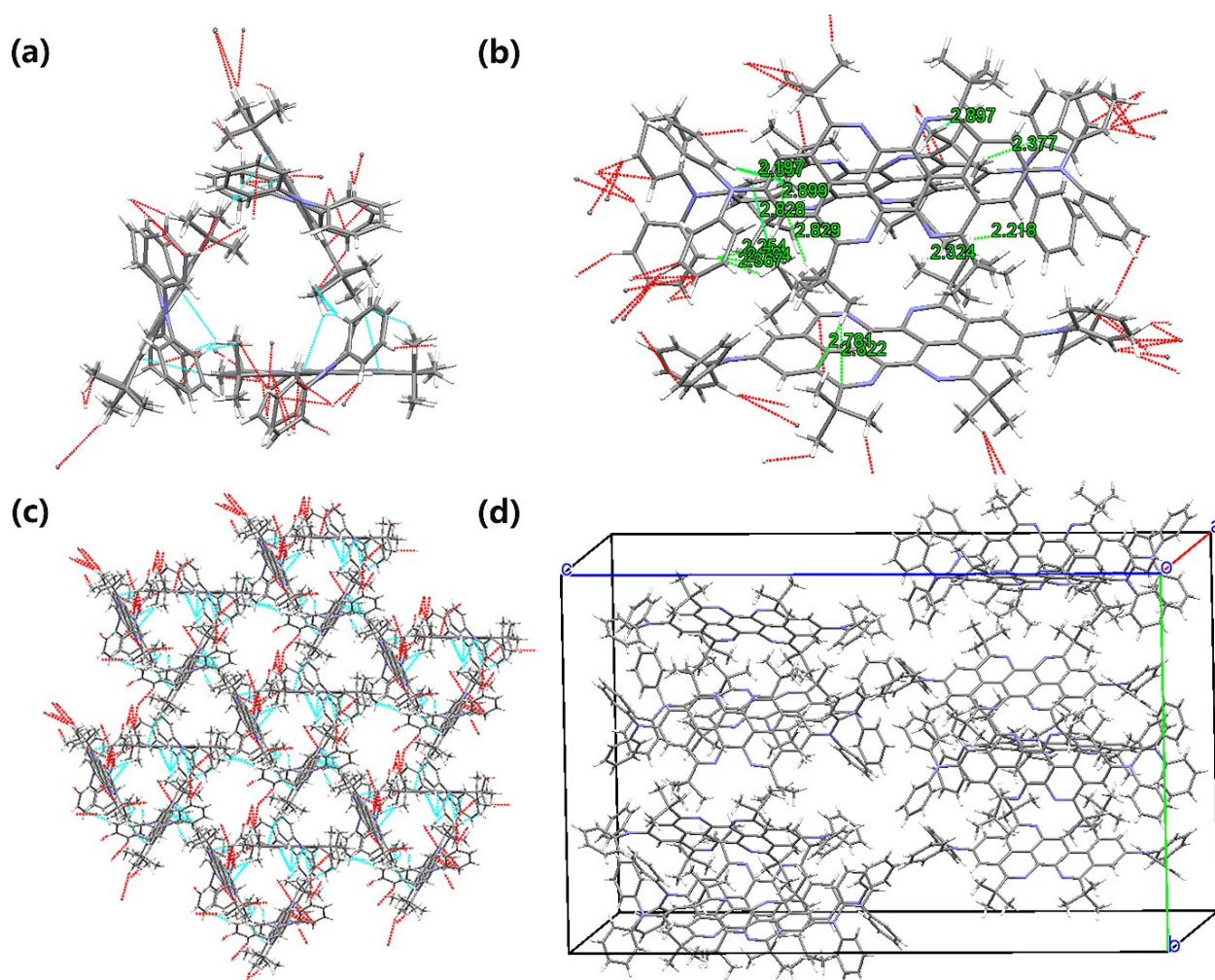


Figure S5. (a), (b) Multiple intermolecular interactions and (c), (d) the molecular packing arrangement of 2D hexagonal microplate.

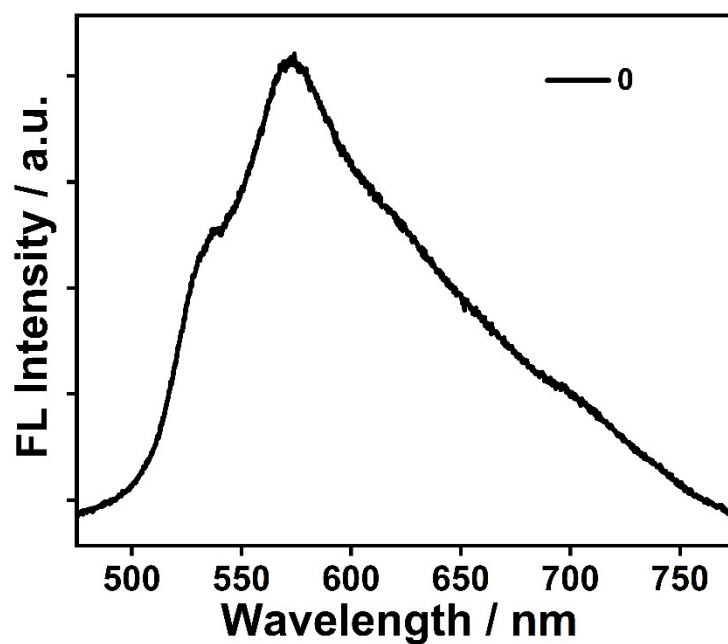


Figure S6. Spatially resolved FL spectra of the excited spot (marked with 0) of the 2D rhomboid microplate of c-TAPP-DPA shown in Figure 4a1.

Table S2. Crystal data of 1D microrod (CCDC: 2237822).

Formula	$C_{62}H_{60}N_6$
Space group	P
Cell lengths	$a/\text{\AA}$ 9.9202 (6), $b/\text{\AA}$ 12.9263 (9), $c/\text{\AA}$ 13.4432 (5)
Cell angles	$\alpha / ^\circ$ 105.07 (6), $\beta / ^\circ$ 93.83 (5), $\gamma / ^\circ$ 110.11 (6)
Cell volume	1539.73
Z, Z'	Z: 1 Z': 0
R-Factor (%)	6.61

Table S3. Crystal data of 2D rhomboid microplate (CCDC: 2237823).

Formula	$C_{62}H_{60}N_6$
Space group	P
Cell lengths	$a/\text{\AA}$ 9.9429 (4), $b/\text{\AA}$ 11.5333 (9), $c/\text{\AA}$ 12.8602 (11)
Cell angles	$\alpha / ^\circ$ 115.500 (8), $\beta / ^\circ$ 91.224 (5), $\gamma / ^\circ$ 91.154 (5)
Cell volume	1330.07
Z, Z'	Z: 2 Z': 0
R-Factor (%)	11.45

Table S4. Crystal data of 2D hexagonal microplate (CCDC: 2237824).

Formula	C ₆₂ H ₆₀ N ₆
Space group	Cc
Cell lengths	a/Å 15.7575 (7), b/Å 27.3445 (13), c/Å 42.700 (3)
Cell angles	α /° 90, β /° 98.010 (6), γ /° 90
Cell volume	18219.1
Z, Z'	Z: 78 Z': 0
R-Factor (%)	11.02

NMR spectra

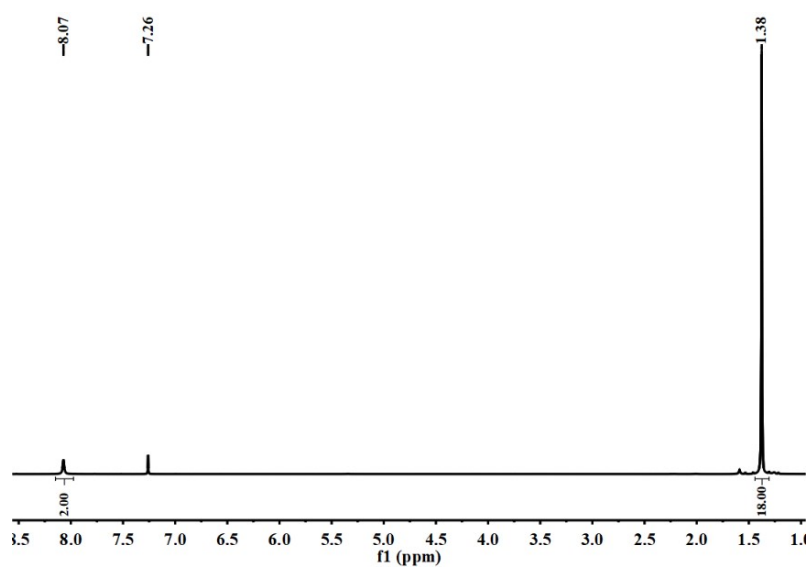


Figure S7. ¹H NMR spectrum of **1** in CDCl₃.

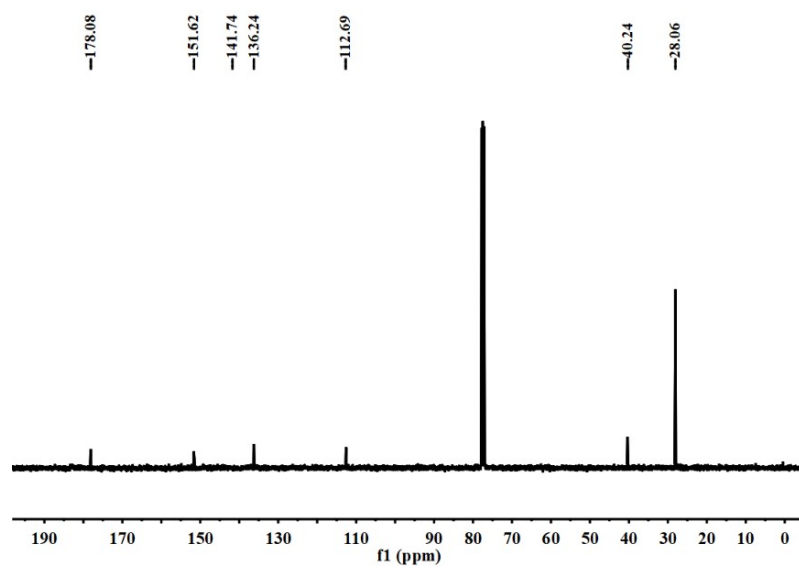


Figure S8. ¹³C NMR spectrum of **1** in CDCl₃.

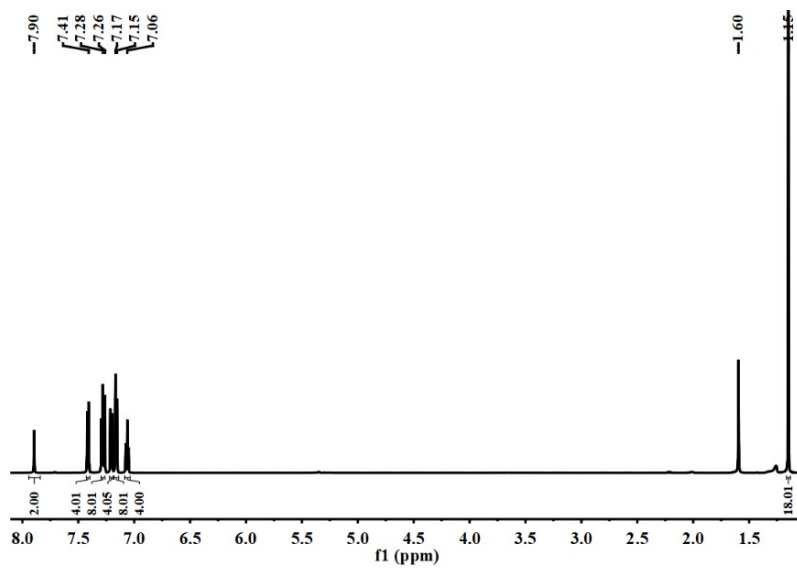


Figure S9. ^1H NMR spectrum of **2** in CDCl_3 .

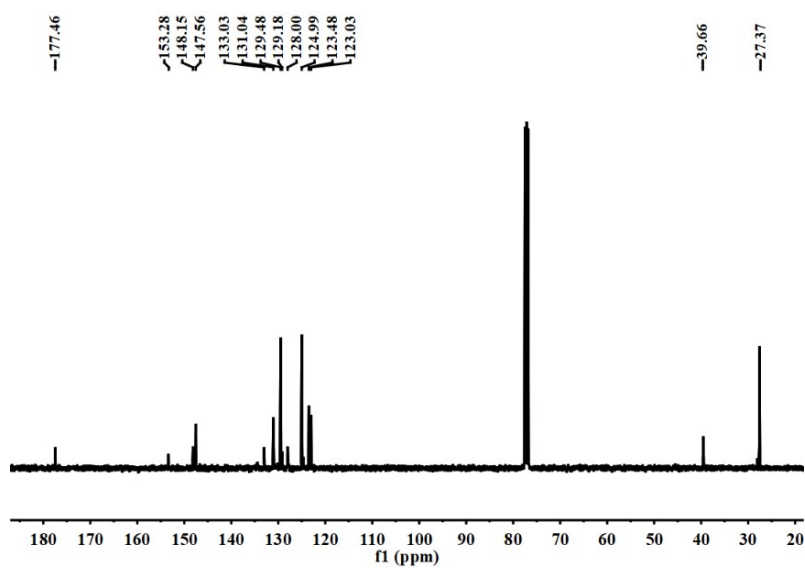


Figure S10. ^{13}C NMR spectrum of **2** in CDCl_3 .

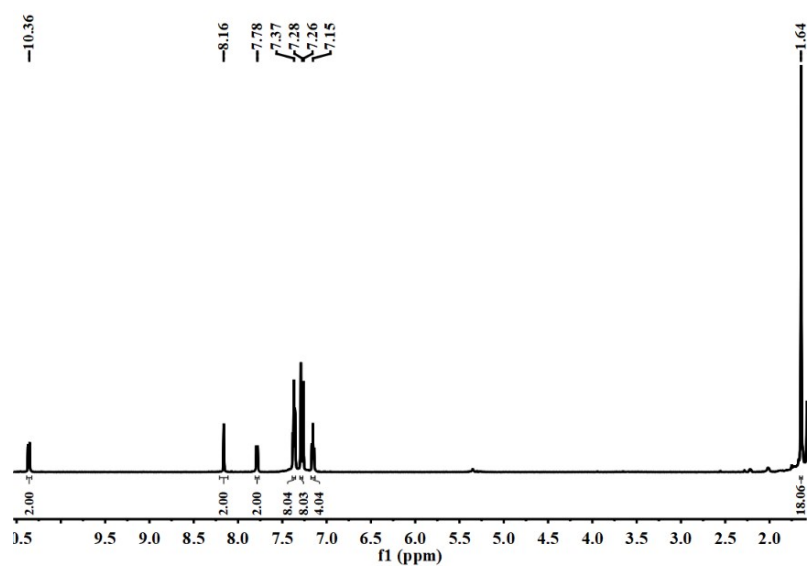


Figure S11. ^1H NMR spectrum of **3** in CDCl_3 .

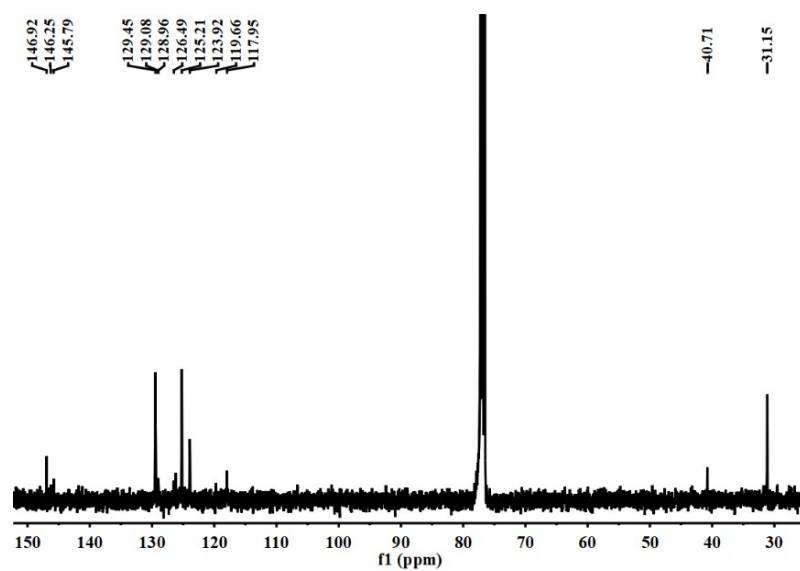


Figure S12. ^{13}C NMR spectrum of **3** in CDCl_3 .

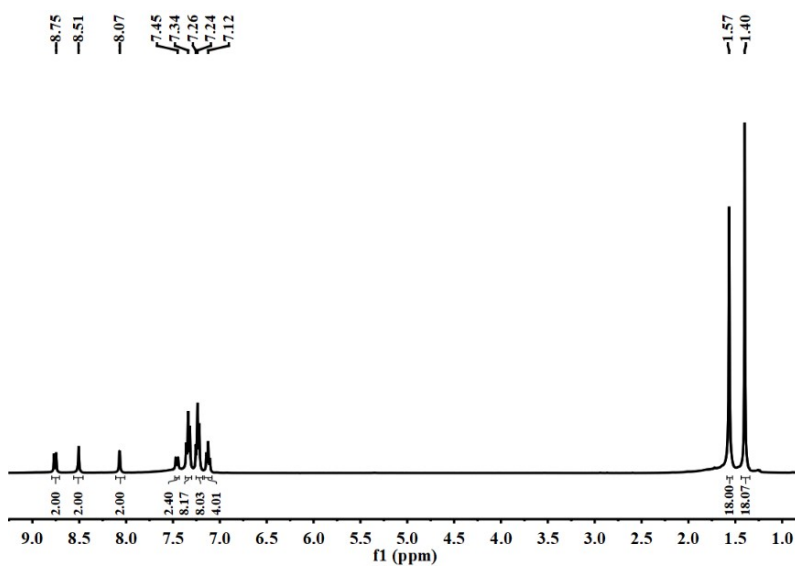


Figure S13. ^1H NMR spectrum of **5** in CDCl_3 .

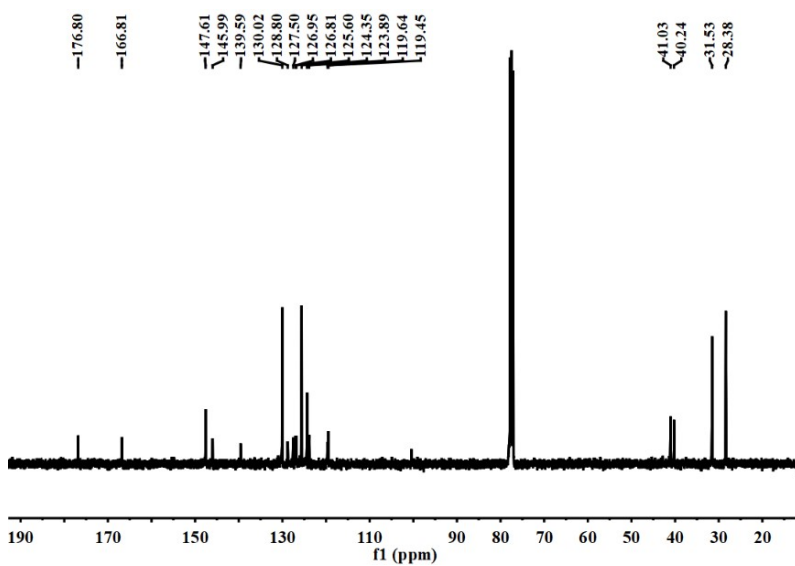


Figure S14. ^{13}C NMR spectrum of **5** in CDCl_3 .

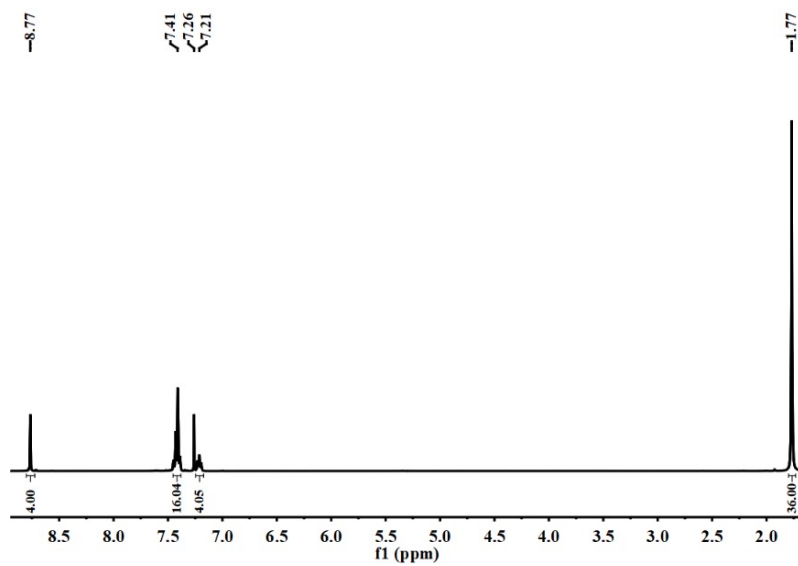


Figure S15. ^1H NMR spectrum of c-TAPP-DPA in CDCl_3 .

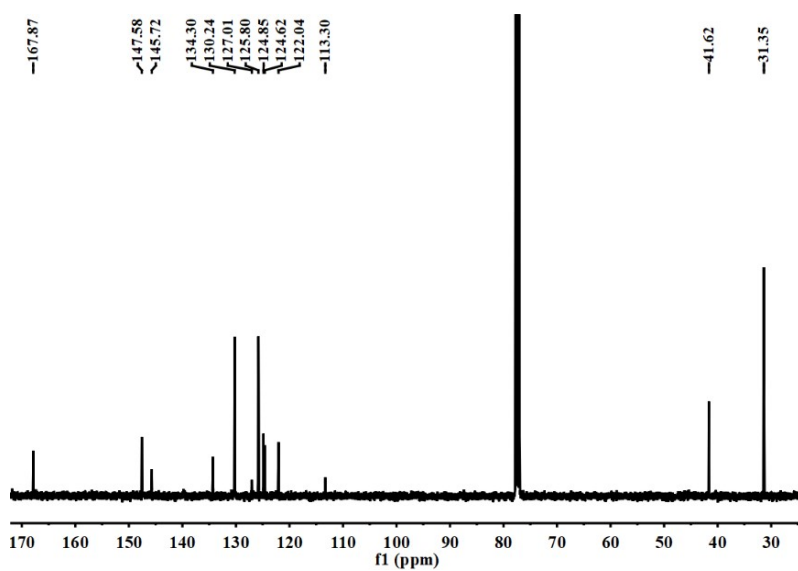


Figure S16. ^{13}C NMR spectrum of c-TAPP-DPA in CDCl_3 .

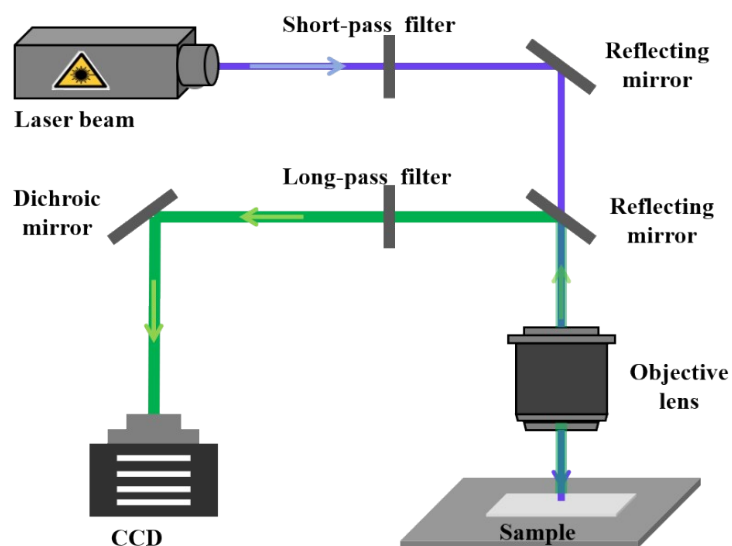


Figure S17. Schematic demonstration of the experimental setup for optical waveguide characterization. To measure the PL spectra of the microcrystals, samples were excited locally with a 375 nm focused beam laser. The power at the input was altered by the neutral density filters. The emission from the tip/edge of microcrystals were dispersed with a grating and recorded with a thermal-electrically cooled CCD.

References

- [1] a) Li, S., Yin, C. F., Wang, R. N., Fan, Q. L., Wu, W., Jiang, X. Q., *ACS Appl. Mater. Interfaces* **2020**, *12*, 20281; b) Song, X. X., Yu, H. B., Yan, X. J., Zhang, Y. W., Miao, Y., Ye, K. Q., Wang, Y., *Dalton T.* **2018**, *47*, 6146.